Journal of Non-Crystalline Solids 356 (2010) 2315–2322

Contents lists available at ScienceDirect

Journal of Non-Crystalline Solids

journal homepage: www.elsevier.com/ locate/ jnoncrysol

First investigations of the influence of IVB elements (Ti, Zr, and Hf) on the chemical durability of soda-lime borosilicate glasses

Boris Bergeron [a,*], Laurence Galoisy [b], Patrick Jollivet [a], Frédéric Angeli [a], Thibault Charpentier [c], Georges Calas [b], Stéphane Gin [a]

[a] CEA DEN, Marcoule, Laboratoire d'Étude du Comportement à Long Terme des Matrices de Conditionnement, BP 17171, 30207 Bagnols-sur-Cèze Cedex, France
[b] Institut de minéralogie et de physique des milieux condensés, UMR CNRS 7590, Université Pierre et Marie Curie, Université Paris Diderot and IPGP, 4 place Jussieu 75005 Paris, France
[c] CEA, IRAMIS, SIS2M, Laboratoire de Structure et Dynamique par Résonance Magnétique, CEA-CNRS UMR 3299, 91191 Gif-sur-Yvette, France

ARTICLE INFO

Article history:
Received 16 October 2009
Received in revised form 15 July 2010
Available online 31 August 2010

Keywords:
Chemical durability;
Corrosion;
Glasses;
Borosilicates;
Silicates;
Surfaces and interfaces;
Nuclear glasses

ABSTRACT

The influence of IVB elements (Zr, Ti, and Hf) on the glass structure and on the alteration kinetics of soda-lime borosilicate glasses has been studied at various stages of glass leaching corresponding to the initial dissolution rate, rate drop, and residual rate regimes. The effect of these elements on the limiting mechanisms of the glass durability as well as the chemistry of both solution and alteration layer are interrelated, depending on the reaction progress. The effect of IVB elements on the glass structure was investigated using ^{11}B MAS NMR. The IVB elements are compensated primarily by Na rather than Ca, at the expense of tetracoordinated boron. The addition of HfO_2 or ZrO_2 decreases the initial dissolution rate in a similar way. Moreover, adding ZrO_2 limits the rate drop in saturated media. The initial dissolution rate decrease is less significant when Ti is added, and a quick drop of the dissolution rate is observed up to 4 mol% TiO_2. At low IVB element concentration, glasses containing Ti and Zr show different residual rates arising from the precipitation of magadiite ($Na_2Si_{14}O_{29}\cdot 11H_2O$), at the surface of Ti-bearing glasses. The influence of IVB elements on glass alteration indicates that, unlike Ti, Zr and Hf plays a similar role in the structure of borosilicate glasses.

1. Introduction

Glass durability is a major issue for the vitrification of high-level nuclear wastes. In the perspective of a deep geological disposal, it is of primary importance to understand the mechanisms of glass alteration by water, in order to model the long-term behavior of nuclear glasses. The rate of glass dissolution depends on variables such as temperature, pH and chemical composition of both glass and alteration solution. The formation of an altered layer (commonly known as 'gel') during the alteration of borosilicate glasses by water accounts for a drop in the glass dissolution rate. In addition, this gel develops retention properties with respect to some glass components that must be taken into account in the calculation of the source term, i.e. the flux of radionuclides released from the glass [1].

The early stages of glass leaching, called "interdiffusion", correspond to a fast ion exchange involving mobile glass components (Na,...) and protons from the solution [2,3]. At the same time, the hydrolysis of the glassy network begins at a lower rate, modifying the Si–O–(Si, Al, Zr…) bonds. The difference between the kinetics of these two simultaneous processes leads to the formation of a porous and hydrated layer at the glass/water interface [3–5]. The release of mobile elements is rapidly controlled by the kinetics of alteration of the silicate glassy network, as protons cannot diffuse deeply into the bulk glass. The glass dissolution rate under these conditions, known as the initial dissolution rate or forward rate, is 2.2 g $m^{-2} d^{-1}$ (0.79 μm d^{-1}) at 90 °C at pH = 8 for the inactive surrogate (SON68) of the French R7T7 nuclear glass [6]. Interdiffusion and hydrolysis processes progressively increase the concentration of sparingly soluble glass components (Si, Zr, Al, Ca, etc.) and the resulting reorganization of the silicate framework leads to the formation of a "gel". The gel formation is accompanied by a drop in the glass dissolution rate. This rate drop, $r(t)$, can be described by coupling between an affinity term related to the approach to equilibrium between the gel and solution[7], and the water diffusion through the gel [8]. The gel acts as a diffusive barrier against the release of mobile elements. Recently, the clogging of the gel porosity of a five-oxide borosilicate glass at the gel/solution interface has been related to the gradual decrease by several orders of magnitude of the dissolution rate [9,10].

When the leachate is saturated with respect to the gel components, the glass continues to be altered at a very low rate, called residual rate. The mechanisms controlling the alteration kinetics at this stage are water diffusion in the gel [11] and – in the case of complex glasses – the formation of secondary crystalline phases incorporating elements from the gel [12].

* Corresponding author. Tel.: +33 4 66 79 63 73; fax: +33 4 66 79 66 20.
E-mail addresses: boris.bergeron@cea.fr (B. Bergeron), patrick.jollivet@cea.fr (P. Jollivet).

0022-3093/$ – see front matter © 2010 Elsevier B.V. All rights reserved.
doi:10.1016/j.jnoncrysol.2010.07.065

The alteration kinetics is highly dependent on the glass chemical composition. Among glass components, Zr has a peculiar influence on the alteration mechanisms of both simplified borosilicate glasses [13] and SON68 glass [14,15]. In both types of glasses, Zr modifies the local and mesoscopic structure, morphology and physicochemical properties of the gel. Increasing the Zr concentration in the glass decreases the short-term glass dissolution kinetics, but leads to a slower decrease of the dissolution rate in saturated conditions [10]. High concentrations of Zr seem to prevent the clogging of the gel porosity [9].

The purpose of the present study is the comparison of the influence on glass dissolution kinetics of various concentrations of Zr and of two other IVB elements, Ti and Hf, in soda-lime borosilicate glasses. In addition to their chemical similarity, some of these elements are of particular interest. For instance, Hf is often used as an inactive surrogate of tetravalent actinides such as Pu(IV) and is an efficient neutron absorber. ZrO_2, TiO_2 and HfO_2 may be incorporated in borosilicate glasses and their solubility is enhanced by a higher concentration of alkaline earths in the glass [16,17]. These three elements also share a low solubility in water [18,19], with solubility products as low as 10^{-55} for "amorphous" HfO_2. Spectroscopic studies have determined the sites occupied by IVB elements in glasses. Zr occurs in a regular octahedral coordination in borosilicate glasses [20] and SON68 glass [14,21], with cations playing a charge-compensating role, thus ensuring the connectivity of $^{[6]}$Zr sites with the borosilicate network. Borosilicate glasses show the presence of $^{[5]}$Ti and $^{[6]}$Ti when they contain non-bridging oxygen atoms (NBO) [22]. $^{[5]}$Ti has 4 bonds with the silicate network, the fifth Ti neighbor being a non-bridging oxygen [23,24]. The Hf–O distances are similar to the Zr–O distances in borosilicate glasses [25]. Due to similar ionic radii of Zr(IV) and Hf (IV), the presence of $^{[6]}$Hf in borosilicate glasses is then favored. These structural properties explain the alkali-enhanced solubility of IVB elements in glasses, alkali cations charge-compensating these elements in low-coordinated sites. It has been recently shown that, in the event of a deficit in charge-compensating cations, elements such as Zr adopt higher coordination sites in order to comply with the Pauling rules and oxygen neighbor neutrality [26].

In this study, borosilicate glasses with ZrO_2, TiO_2 and HfO_2 concentrations ranging from 1 to 8 mol%, were synthesized in order to compare the influence of the nature and concentration of a IVB element on glass leaching during the initial dissolution rate, rate drop and residual rate regimes. Glasses were obtained from a $61SiO_2$–$17B_2O_3$–18 Na_2O–4CaO glass composition by replacing SiO_2 by ZrO_2, TiO_2 or HfO_2. The influence of charge compensation was investigated by a further replacement of Na_2O by CaO. Glass samples are referred to as M_xC_y, where M refers to the IVB element (Z for Zr, T for Ti, and H for Hf), C stands for CaO and x and *y* correspond to the molar concentrations, $0C_y$ designing the M-free glass. Glasses compositions are reported in Table 1, along with the reference glass without IVB element. The $^{[4]}$B/$^{[3]}$B ratio in the glasses was determined by ^{11}B MAS NMR with different Zr, Ti, and Hf concentrations. Relative to the 0C4 glass, this ratio decreases significantly with increasing MO_2 content, further replacement of Na_2O by CaO providing a further decrease in Hf- and Zr-bearing glasses. This may be related to different coordination geometries of Ti relative to Zr and Hf in these glasses. The initial dissolution rate decreases significantly with increasing MO_2 contents for Hf- and Zr-bearing glasses, but the presence of TiO_2 does not give such a clear trend. Zr and Ti-bearing glasses have been also investigated in the rate drop residual alteration regime. The lowest resistance to hydrolysis corresponds to the quickest drop of their dissolution rate. In residual rate regime, the measured kinetics is of one order of magnitude lower than the residual rate measured for SON68 glass. The replacement of Na_2O by CaO, as shown in the Z8C8 glass, enhances the long-term durability. This may arise from the presence of zirconosilicate associations in the gel, in relation with the formation of $^{[6]}$Zr, efficiently charge-compensated by Ca. By contrast, the faster long-term dissolution rate of T1C4 relative to Z1C4 glass arises from the precipitation of magadiite ($Na_2Si_{14}O_{29}\cdot 11H_2O$) at the surface of the former.

Table 1
Analyzed compositions of the studied glasses.

Glass	Composition of the glass (Oxide mol%)						
	SiO_2	B_2O_3	Na_2O	CaO	ZrO_2	TiO_2	HfO_2
0C4	61.4	16.9	18.1	3.6	–	–	–
Z1C4	61.3	15.9	18.3	3.5	1.0	–	–
T1C4	60.8	16.8	17.8	3.6	–	1.0	–
H1C4	61.9	15.7	17.7	3.7	–	–	1.0
Z4C4	56.7	17.9	18.0	3.7	3.9	–	–
T4C4	57.2	17.1	18.0	3.8	–	3.9	–
H4C4	57.9	17.7	17.7	3.9	–	–	3.9
Z8C4	51.7	17.9	18.6	3.8	8.0	–	–
T8C4	55.8	17.1	14.7	3.8	–	8.6	–
H8C4	53.5	16.1	18.1	3.9	–	–	8.4
Z8C8	52.5	16.9	14.5	8.0	8.1	–	–
T8C8	53.2	16.4	14.0	8.3	–	8.1	–
H8C8	52.8	16.1	14.5	8.3	–	–	8.3

2. Experimental

2.1. Glass synthesis

The twelve glasses were prepared by mixing suitable amounts of reagent grade SiO_2, H_3BO_3, Na_2CO_3, CaO, ZrO_2, TiO_2, or HfO_2. The mixtures were melted in a platinum crucible for 3 h at 1300 °C, poured into a preheated graphite crucible and annealed for 1 h at 600 °C. The glasses compositions were analyzed using X-Ray Fluorescence by the AREVA-NC Marcoule DEX/LAB laboratory (Table 1). Relative uncertainty on the molar percentage of oxide is 5%. Glass specimens were ground in a tungsten carbide planetary ball mill and sieved to recover the 20–40 μm and 5–10 μm powder size fractions. These glass powders were washed in acetone to remove the fine particles formed during the grinding process. The specific surface area of the two fractions was measured for each glass by krypton adsorption using the Brunauer–Emmett–Teller (BET) method. The specific surface areas were 0.18 ± 0.02 $m^2 g^{-1}$ and 0.68 ± 0.10 $m^2 g^{-1}$ for powder of the 20–40 μm and the 5–10 μm fractions respectively. The relative uncertainty on the measurement of the specific surface area is 5%.

2.2. ^{11}B MAS NMR

Boron coordination was determined in the pristine glasses by ^{11}B MAS NMR ($I = 3/2$,). Spectra were collected at 11.72 T (Larmor frequency $\nu_o = 160.14$ MHz) on a Bruker Avance II 500WB spectrometer with a spinning frequency of 12.5 kHz (4 mm o.d. rotor). A single short pulse of 1 μs (π/12) and recycle delay of 2 s were used to ensure that intensity of a peak is linearly linked to its contribution proportion [27]. Chemical shifts were referenced to an external sample of 1 M (19.6 ppm) boric acid solution. The proportions of $^{[4]}$B and $^{[3]}$B sites were quantified using a procedure described in details in [28]. The central region of the spectrum corresponding to the central transition (−½ ↔ ½) was corrected for the contribution of satellite transitions by subtracting the first spinning sideband from the central band [27].

2.3. Leaching procedures

Initial dissolution rates were measured in deionized water at 90 °C ± 2 °C using single-pass flow-through (SPFT) experiments [29]. The SPFT device consists of a polytetrafluoroethylene (PTFE) reaction cell, in which an open circulation of deionized water (MilliQ 18.2 MΩ cm) reacts with

the glass at a constant temperature and rate. The mass of the 20–40 μm glass powder fraction was adjusted to obtain a flow rate (Q) per unit glass surface area (SA) corresponding to $log_{10}\ Q/SA \approx -4.9$ m s^{-1}. The small size of the reaction cell (around 1 cm^3) and the high flow rate ensure solution renewal in less than 10 s. The leachate was regularly sampled and the Si concentration determined by colorimetry with a Merck Spectroquant® kit.

Rate drops were measured by static experiments in PTFE reactors placed in an oven regulated at 90 ± 2 °C. The 20–40 μm glass powder fraction was contacted with 250 cm^3 of solution for Zr-bearing glasses, as well as for T1C4 and T4C4. The 5–10 μm fraction was used for the other glasses. The mass of each glass powder sample was adjusted to obtain a glass surface area to solution volume (SA/V) ratio of 15 cm^{-1}. The alteration solution was buffered at $pH_{90\ °C} = 7.0 \pm 0.1$ using a solution of 0.2 M TRIS (Tris-hydroxymethyl aminomethane) and 0.1 M HNO_3. Samples of the output solutions were filtered to 0.45 μm, diluted and acidified to 1% HNO_3 (65% Merck SupraPur).

A second kind of static leaching experiments was also carried out on Zr-containing glasses and T1C4 glass samples to determine the effect of Zr and Ti on the residual leaching rate. The glass powder was placed in PTFE reactors and leached in 30 cm^3 of deionized water at 90 °C. The glass quantity was adjusted for a SA/V ratio of 2000 cm^{-1}. Small solution samples (0.3 mL) were sampled, filtered to 0.45 μm, diluted, and acidified to 1% HNO_3 (65% Merck SupraPur®).

2.4. Chemical analysis

The leaching solution was analyzed by ICP-AES using a Jobin Yvon JY 66 P spectrometer to determine the Si, B, Na, Ca, Zr and Ti concentrations. Leaching solutions of the Hf glass series were analyzed by ICP-MS using a Thermo-fisher X 7 (Central Analysis Service, SCA-CNRS) to determine the Si, B, Na, Ca, and Hf concentrations. Uncertainties on the determination of the element concentration in solution and in the glass are 5% in relative value.

2.5. Scanning Electron Microscopy (SEM) and X-ray diffraction (XRD)

The glass powders leached at a SA/V ratio of 2000 cm^{-1} at 90 °C were sampled after 600 days of leaching and washed at room temperature in deionized water to dilute the alteration solution residue. The powders were dried at 40 °C for 12 h and then at 90 °C for 1 day. A thin carbon layer was sputtered on the samples. Samples were analyzed on a ZEISS Supra 55 SEM fitted with a Brucker Quantax Energy-Dispersive Spectrometer (EDS). Observations were performed at 5.0 kV with a beam current of 200 nA, and EDS spectra were acquired at 15 kV. XRD was performed with Cu Kα radiation on a Panalytical X'Pert equipped with an X'Celerator detector and operating at 40 kV and 40 mA.

3. Results and discussion

3.1. ^{11}B NMR MAS investigation of boron coordination in pristine glasses

Fig. 1a shows the ^{11}B MAS NMR spectra for glass containing Hf and Ti. The spectra present two main bands that are related to $^{[3]}$B and $^{[4]}$B. The broader band centered around 11 ppm corresponds to 3-coordinated boron ($^{[3]}$B) characterized by a quadrupolar coupling constant C_Q higher than $^{[4]}$B boron. This contribution is attributable to the presence of two sites: boron surrounded by bridging bonds in boroxol rings (BO_3 ring) and boron distributed in silicate units (BO_3 non-ring) [29]. The increase of the TiO_2 and HfO_2 content leads to an increase of the $^{[3]}$B contribution. In the same glasses, the $^{[4]}$B band slightly shifts to higher chemical shift values with the increase of the TiO_2 and HfO_2 content. Different $^{[4]}$B surroundings can contribute to the $^{[4]}$B band as recently shown in soda-lime borosilicate glasses

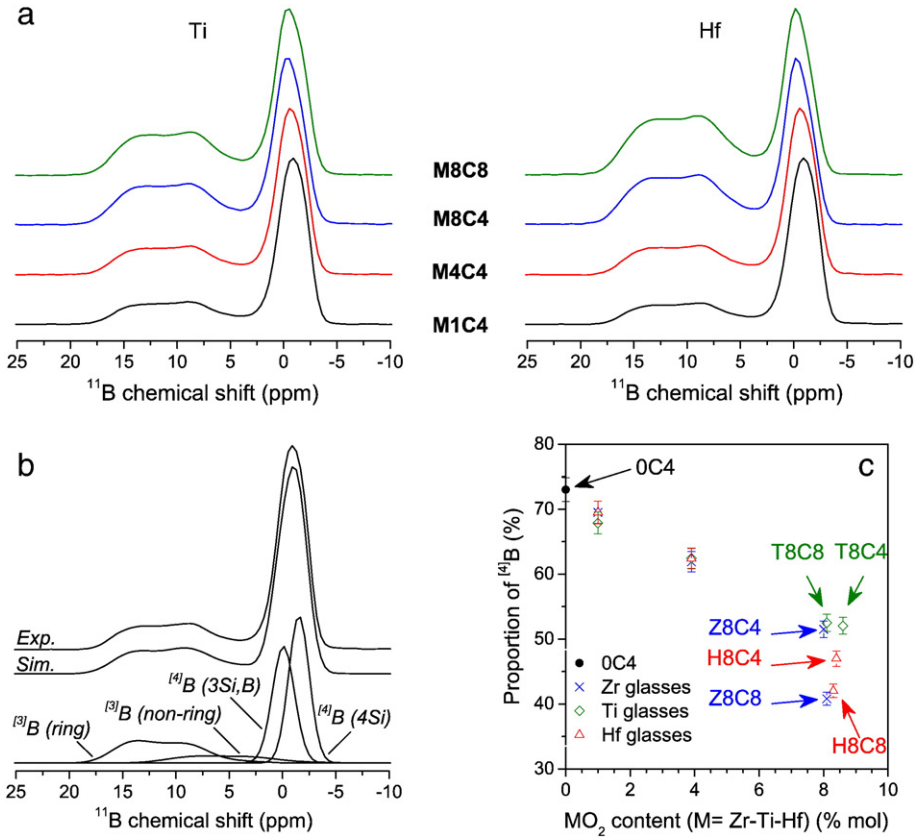

Fig. 1. (a) ^{11}B MAS NMR spectra of Ti and Hf-bearing glasses. (b) Example of decomposition of 11B MAS NMR spectrum in H1C4 glass (see text for details). (c) Proportion of $^{[4]}$B derived from ^{11}B MAS NMR for the different glasses investigated, showing the strong influence of the concentration of IVB elements.

[30,31]. The NMR signals relative to tetrahedral borate groups surrounded either by four Si ($^{[4]}$B(0B, 4Si)) or by three Si and one B ($^{[4]}$B(1B, 3Si)) are located at −2 and 1 ppm, respectively [32] The slight shift of the $^{[4]}$B peak towards higher values with increasing the MO_2 content indicates a lower contribution of $^{[4]}$B(0B, 4Si).

The fraction of $^{[4]}$B (N4) was quantified from the respective area of each component. Fig. 1b shows the variation of N4 with MO_2 content. N4 values for our Zr-bearing glasses and for the 0C4 glass have been recently published [30] and are reported in this figure for comparison. The chemical dependence of N4 has been investigated in SiO_2–B_2O_3–Na_2O glasses and rationalized as a function of $R = Na_2O/B_2O_3$ and $K = SiO_2/B_2O_3$ ratios [31]. Using this model, the K and R ratios of the 0C4 glass indicate a N4 value of 73%, i.e. the experimental value. The presence of additional Ca^{2+} cations in the glass does not influence boron coordination in this glass containing high content of Na_2O.

The addition of ZrO_2, TiO_2, or HfO_2 leads to a decrease of the proportion of $^{[4]}$B by 15–20% relative to 0C4. Such a decrease cannot be rationalized by the slight decrease of the SiO_2 content with the addition of IVB elements, as the Dell model would suggest [31]. However, the glasses with 1 to 4 mol % MO_2 contain a proportion of cations (Na_2O + CaO) able to charge-compensate $^{[4]}$B as well as $^{[6]}$Zr, $^{[6]}$Hf, $^{[5]}$Ti or $^{[6]}$Ti (Table 1). Our results indicate a competition for charge compensation by Ca or Na between $^{[4]}$B and the IVB elements, a process already described in borosilicate glasses containing elements able to adopt various coordination geometries, such as Zr or Al [33]. The decrease of N4 when CaO replaces Na_2O in the glasses with 2 mol% ZrO_2 confirms that $^{[4]}$B is preferentially compensated by Na^+ [30]. However Na^+ also compensates preferentially $^{[6]}$Hf, $^{[5]}$Ti and $^{[6]}$Ti, like $^{[6]}$Zr, rather than $^{[4]}$B. As Ca does not play an efficient charge-compensating role for $^{[4]}$B, N4 decreases from M8C4 to M8C8 in Zr- and Hf-bearing glasses. By contrast, N4 remains constant in Ti-containing glasses, T8C4 and T8C8 despite the addition of 4 mol% CaO in T8C8.

For 1 and 4 mol% IVB element and 8 mol% Zr and Hf, the similar N4 values indicate a similar local environment of IVB elements. N4 is similar in T8C4 and Z8C4, despite a lower Na_2O concentration in T8C4. Moreover, T8C8 presents a higher proportion of $^{[4]}$B than Z8C8 and H8C8. It may be inferred by the presence of $^{[5]}$Ti in T8 glasses, which requires less charge compensation than $^{[6]}$Zr and $^{[4]}$Hf in the corresponding samples.

3.2. Initial dissolution rate

The value of the initial dissolution rate r_0 (Fig. 2) is deduced from the Si concentration in the leachate of the SPFT experiment during the first three hours of alteration from the following relation (1):

$$r_0 = \frac{C_{Si} \times \frac{Q}{SA}}{f_{Si}} \quad (1)$$

where C_{Si} is the silicon concentration in the alteration solution (mg L^{-1}), f_{Si} is the weight fraction of Si in the glass, and Q/SA is the flow rate (Q) per unit glass surface area (SA). Uncertainty on the r_0 was calculated according to the uncertainty propagation law by assuming that the measurements are independent. Si concentration in the alteration solution remains below 5.5 mg L^{-1}, less than 4% of the Si concentration at saturation under static experiments at $pH_{90\,°C} = 7.0$ described below. Glass dissolution in such diluted conditions avoids any feedback effect of the dissolved elements on the alteration kinetics. The alteration remains congruent, ensuring an accurate determination of r_0 with the dissolved SiO_2 concentration.

The r_0 of the 0C4 glass is 51 g m^{-2} d^{-1}. This rate is higher than the r_0 values in IVB element containing glasses. Due to this high r_0 value, the water flow rate was increased to prevent a limiting effect of the dissolved elements on dissolution kinetics ($Q/SA = 2$ m d^{-1}).

3.2.1. Zr-bearing glasses

In these SPFT leaching experiments, Z1C4 presents a r_0 of 34 g m^{-2} d^{-1}. This value drops to 4.0 g m^{-2} d^{-1} when the ZrO_2 content increases from 1 to 8 mol%. The addition of 1 mol% ZrO_2 in the glass composition substantially increases its resistance to hydrolysis, but further increase in the ZrO_2 content to 8 mol% does not induce such an increase of the resistance. The correlation between the r_0 decrease and the ZrO_2 content is in agreement with previous leaching studies with similar glasses in diluted static conditions [10]. In reference [10], r_0 values decrease from 37 to 0.091 g m^{-2} d^{-1} when ZrO_2 content varies from 0 to 8 mol%. These r_0 values are smaller than in our study. This difference can be explained by the use of different leaching protocols. SPFT experiment maintain a low Si concentration at the glass/solution interface by ensuring an adequate dilution of the solution, whereas leaching under static condition leads to a small increase of SiO_2 concentration with the dissolution progress.

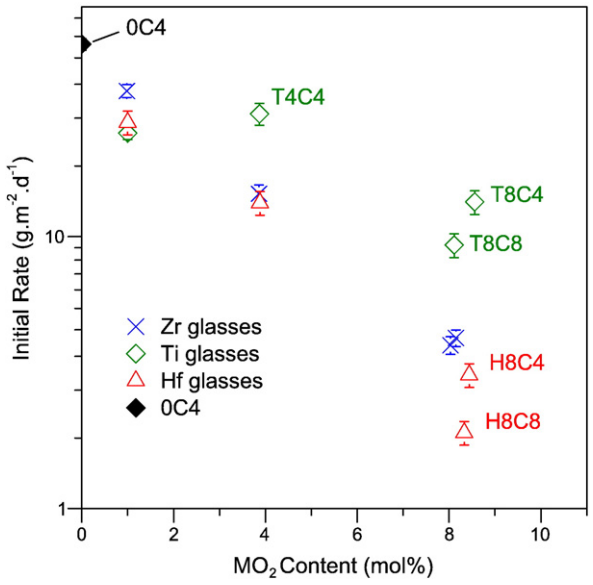

Fig. 2. Evolution of the initial dissolution rate at T° = 90 °C in function of the IVB element concentration. The initial dissolution rate of the 0C4 glass containing no IVB element was determined at $Q/SA = 2$ m d^{-1}.

3.2.2. Hf-bearing glasses

The glass containing 1 mol% HfO_2 presents a r_0 twice lower than the 0C4 glass (26 g m^{-2} d^{-1}). As for Zr-containing glasses, further addition of HfO_2 induces a decrease in the r_0. For the same composition, the rate for Hf-bearing glass is however lower than for Zr-bearing glass (26 to 3.0 g m^{-2} d^{-1}). The similar effect of Zr and Hf on r_0 can be related to the similar chemical properties and local environment of this two elements in borosilicate glasses [21,25]. The lower r_0 values observed for glasses containing HfO_2 could be due to the slightly lower Na_2O content of Hf-bearing glasses compared to the Zr-containing glasses. Addition of Na_2O increases the depolymerisation of the silicate network and leads to an increase of the r_0 [34].

3.2.3. Ti-bearing glasses

The r_0 value of the T1C4 (24 g m^{-2} d^{-1}) is twice lower than for the 0C4 glass. Contrarily to ZrO_2 and HfO_2, the increase of TiO_2 content up to 4 mol% induces an increase of r_0 values up to 28 g m^{-2} d^{-1}. For T8C4, the r_0 value is 13.4 g m^{-2} d^{-1}. As this sample has a Na_2O deficit with respect to the composition of the other M8C4 glass samples, the decrease of the r_0 cannot be exclusively attributed to a higher TiO_2 content (Table 1). With 4 and 8 mol% of IVB elements, the dissolution rate for Ti-bearing glasses is nevertheless higher than for the equivalent Zr- and Hf-bearing glasses. ^{11}B MAS NMR experiment showed that Ti could have a lower coordination in glasses containing 8 mol% TiO_2. The decrease of the Ti coordination decreases the number of bonds between Ti and the silicate network and could induce a lower effect of this element on the r_0 compared to Zr and Hf.

3.2.4. Origin of the chemical dependence of r_0

Due to the high level of dilution, the leaching conditions prevent any formation of a protective gel. The variation among the r_0 values for the different glasses corresponds to the resistance of the silicate network to hydrolysis. The decrease of the kinetics of alteration resulting from the substitution of SiO_2 by ZrO_2 is in agreement with previous studies on borosilicate glasses with simplified compositions belonging to the SON68 composition range [34]. Different models have attempted to predict the variation of r_0 according to the glass composition by relating the dissolution rate to thermodynamic data. The model proposed by Feng and Barkatt [35,36] established a relation between the resistance to hydrolysis and the strength of the glass network, considered as a weighted sum of the enthalpies of formation of oxides. Paul [37] or Jantzen and Plodinec [38] related the dissolution rate to the free enthalpy of hydration of the glass calculated from the free enthalpy of hydration of reference compounds. The low solubility of zirconosilicate minerals [18,39] and the free energy of formation of zircon and hafnon [40] compared with quartz or amorphous silica [41–43] prove the higher resistance to hydrolysis of the Si–O–Zr bonds in comparison to the Si–O–Si bonds. These models can thus account for the lower dissolution rate, when ZrO_2 or HfO_2 replace SiO_2 as observed in our glasses. However, such models cannot explain the non-monotonic evolution of the dissolution rate with the TiO_2 content in the glass.

The effect of adding CaO differs according to the nature of the IVB element. The increase of the CaO content has no significant effect on r_0 values in Zr-bearing glasses. Z8C4 and Z8C8 present similar r_0 values of 4.0 and 4.2 g $m^{-2} d^{-1}$ respectively. In Hf-bearing glass, addition of CaO results in a drop of the r_0 from 3.1 to 1.9 g $m^{-2} d^{-1}$. Such as Hf-containing glasses, Ti-bearing glasses present a decrease of r_0 values from 13.4 to 9.3 g $m^{-2} d^{-1}$ with the increase of the CaO content.

In Zr and Hf-containing glasses, the different r_0 for M8C4 and M8C8 may be discussed by the different effect of CaO and Na_2O on the resistance of the silicate network to hydrolysis. The increase of CaO content does not change the resistance to hydrolysis of the silicate network in Zr-containing glasses but increases the resistance in Hf-bearing glasses. In Ti-containing glasses, the difference between T8C4 and T8C8 corresponds to an addition of 4 mol% CaO, as the Na_2O content of T8C4 is below the nominal value. The decrease of r_0 between T8C4 and T8C8 show a strengthening of the silicate network with the addition of CaO. In glasses without IVB elements, the presence of CaO increases r_0, whereas, with the additional presence of ZrO_2, this increase is smaller [34]. By contrast, we show that the increase of CaO content in presence of TiO_2 and HfO_2 decreases the r_0.

In the absence of IVB element, the increase of r_0 with CaO content is often associated with the network-modifying role of Ca and the formation in the glass network of non-bridging oxygen atoms (NBO), which favor hydrolysis of the silicate network [34]. ^{11}B NMR shows that replacing Na_2O by CaO decreases the $^{[4]}B$ proportion in glass containing 8 mol% IVB elements and thus increases the concentration of NBOs. Nevertheless, r_0 decreases under the same conditions. Thus, r_0 cannot be directly correlated with the concentration of non-bridging oxygen atoms, and the effect of CaO on r_0 cannot be explained in this way.

The change in the structural role of Ca may account for the effect of CaO on r_0 in glasses containing 8 mol% IVB elements. The Na_2O content of M8C8 glass samples is too low to compensate all the $^{[4]}B$ and IVB elements present in the glass composition. A fraction of the Ca^{2+} must therefore assume a charge-compensating role in M8C8 glasses. However, only a minor amount of Ca^{2+} plays a charge-compensating role in the glass, as IVB elements are preferentially charge-compensated by Na.

The role of CaO on r_0 in the presence of IVB elements can be related to its charge-compensating role not only in the glass, but also in the hydrolysis products. During leaching in a SiO_2-unsaturated medium, Zr tends to change from 6- to 7-coordination in hydrous zirconium oxide (HZO–$Zr(OH)_4$) [14]. The presence of Ca helps in maintaining $^{[6]}$Zr within the silicate network and thus enhances the network resistance to hydrolysis. In alteration experiments where SiO_2 solubility is reached, the presence of ZrO_2 in the glass induces the retention of Ca in the alteration gel [44]. The affinity between Ca and Zr takes place in under-saturated conditions and could explain the r_0 difference between M8C4 and M8C8. Bunker has shown that the diffusion of water in the silicate network depends on the size of the silicate rings [45]. The modification of the medium-range order and thus of the ring distribution by IVB elements and Ca will then directly affect r_0.

3.3. Dissolution rate drop regime (r(t))

Alteration under static conditions at a *SA*/*V* ratio of 15 cm^{-1} reveals the effect of the formation of the gel on the alteration kinetics and raises the issue of the efficiency of different gels as diffusion barriers. In such conditions, the rise of the SiO_2 concentration in solution is followed by SiO_2 retention in the gel layer. The evolution of the Si concentration in solution no more reveals the progress of the alteration of the pristine glass. The progress of the reaction is then measured by the boron concentration in solution. Boron is a good alteration tracer for borosilicate glasses, as it is a network former that is not retained in the alteration products [46]. The quantity of leached glass per unit glass surface area is determined by calculating the normalized mass losses of boron ($NL(B)$):

$$NL(B) = \frac{C_B \times V}{f_B \times SA} \quad (2)$$

where C_B is the boron concentration (mg L^{-1}) in solution of volume *V*, f_B the weight fraction of boron in the glass, and *SA* the surface area of the glass powder in the reactor. Uncertainty mostly arises from the determination of the glass powder specific area and of the element concentration in solution and in the glass. Uncertainties of the $NL(B)$ values were calculated according to the uncertainty propagation law by assuming that the measurements are independent. Fig. 3 shows the evolution of the $NL(B)$ of the twelve glass samples over time. The X-axis is plotted on a logarithmic scale to observe changes in the quantity of altered glass from the initial instants to the end of alteration. The leaching time is 600 days. The experiments were ended when the proportion of altered glass reached 90% (T8C4, T8C8). No shrinking-core model was used to correct the normalized mass losses for the decrease of the reactive glass surface area over time.

3.3.1. Zr-bearing glasses

For all samples, less than 1.2 g m^{-2} of glass has been dissolved after 6 h of leaching, indicating that the dissolution rate decreased by more than one order of magnitude as compared to the initial dissolution rate. After 6 h, the quantity of leached glass decreases with ZrO_2-content (Fig. 3) as observed for r_0. After one day of alteration, the Z1C4 glass dissolution rate dropped very quickly, and further alteration was no longer measurable after seven days. The rate drop decreases drastically when ZrO_2 is added. The quantity of leached glass slowly increases up to 600 days of leaching. The inhibition of alteration observed in glasses containing 1 mol% ZrO_2 has been interpreted as arising from the clogging of the gel porosity at the gel/solution interface [13] as confirmed by Monte-Carlo simulations [10]. The addition of Zr in the glass retains the SiO_2 during hydrolysis and then prevents the rearrangement of the gel that leads to the pore closure [9,10,13].

3.3.2. Ti-bearing glasses

After one day of leaching, the altered glass quantities were similar for T1C4 (1.5 g m^{-2}) and T4C4 (1.7 g m^{-2}). At the same time, the quantity of altered glass for T8C4 was 0.85 g m^{-2} and 0.42 g m^{-2} for T8C8. After one day, the quantity of altered glass varied as the r_0. The alteration of

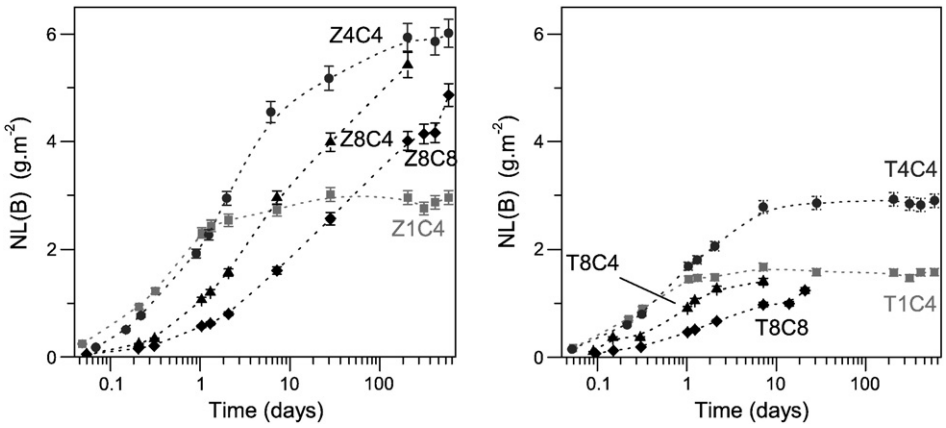

Fig. 3. Evolution of the normalized mass losses of boron for the Zr (a) and Ti-bearing glasses (b) during the alteration at $pH_{90\,°C} = 7$, $SA/V = 15\ cm^{-1}$ and $T° = 90\ °C$.

T1C4 and T4C4 stopped after 1 and 7 days, respectively. Alteration is inhibited more quickly and with smaller quantities of altered glass for T1C4 (1.5 g m^{-2}) than for Z1C4 (2.7 g m^{-2}). On the contrary to Z4C4 that is leached up to 6 g m^{-2} after 600 days, the alteration of T4C4 is stopped at 2.8 g m^{-2}. The quick drop of the alteration during leaching of T1C4 and T4C4 glasses suggests that pore closure also occurs for these glasses. Increasing TiO_2 up to 4 mol% only delays the gel pore closure, on the contrary to ZrO_2 that inhibits porosity clogging. This suggests that Ti inhibits the reorganization of the gel in a less efficient way than Zr. In the samples containing 8 mol% TiO_2, no quick drop of the dissolution rate is detected after 7 days. The Z1C4, T1C4 and T4C4 glasses, in which alteration rapidly stops, are also those with the highest r_0, i.e. with the lowest resistance to hydrolysis. This suggests that the mechanism responsible for the rapid decrease in the kinetics of Z1C4 alteration is also responsible for the rapid decrease of the alteration kinetics of T1C4 and T4C4 glasses. The different behavior of Ti and Zr could be related to their efficiency in retaining Si. A coordination change of Ti during hydrolysis could thus decrease its capacity to retain Si during alteration, and then explain the blocking of the alteration of the T4C4 glass.

3.3.3. CaO content

Even though Z8C8 and Z8C4 present the same r_0, the quantity of altered glass for the Z8C8 (0.20 g m^{-2}) after 6 h is less than for Z8C4 (0.34 g m^{-2}). The quantities of altered glass for Z8C8 remain lower than for Z8C4 glass throughout the whole alteration in the rate drop regime. As in the case of Zr-bearing glasses, the quantity of altered glass is systematically lower for T8C8 than for T8C4. The presence of Ca leads to the formation of a more protective gel. The gel protective properties are not only controlled through SiO_2 retention by IVB elements. The presence of Ca must be taken into account as it can have a major role in the structural reorganization of the gel. During the leaching at $pH_{90\,°C} = 7$ of a soda-lime borosilicate glass, the retention of Ca in the gel takes place near the gel-solution interface, where the closure of the porosity occurs [10]. Ca plays a major role in the condensation–dissolution mechanisms leading to the reorganization of the gel porosity.

3.4. Residual rate (r_r)

Fig. 4 shows the evolution of the normalized mass losses of boron, $NL(B)$, as a function of time during the $SA/V = 2000\ cm^{-1}$ experiments. The high SA/V ratio ($2000\ cm^{-1}$) chosen for this experiment allows the solution to quickly reach saturation, leading to the formation of a protective gel after only a short time (<40 days). During this alteration, it is observed that $NL(B)$ rapidly increases during the first 40 days of leaching, corresponding to the rate drop regime. After this period, $NL(B)$ shows a lower increase and the measured kinetics is of the order of magnitude of the residual rate measured for SON68 glass ($1.7 \times 10^{-4}\ g\,m^{-2}\,d^{-1}$ after one year at $2000\ cm^{-1}$, 90 °C) [6]. Z1C4 and T1C4 glasses appear to have reached a near constant rate whereas the dissolution rate of the other Zr-bearing glasses decreases slightly between 200 and 500 days. The residual rates calculated by linear regression of the evolution of $NL(B)$ between 40 and 500 days are presented in Table 2 with the pH value measured after 532 days of leaching. The $NL(B)$ of SON68 are taken from [12] and the residual rate is recalculated by linear regression of the evolution of the $NL(B)$ between 56 and 539 days. The existence of a residual rate can reveal a possible competition between the formation of a protective gel and the crystallization of secondary phases under suitable thermodynamic conditions.

3.4.1. Zr containing glasses

The increasing ZrO_2 content in glass leads to an increase in the measured residual rate. The residual rate of Z8C4 ($1.2 \times 10^{-4}\ g\,m^{-2}\,d^{-1}$) is four times higher than for Z1C4. At the same time, the pH of the leaching solution decreases from 9.63 to 9.35 when ZrO_2 content increases from 1 to 8 mol%. The absence of secondary phases during

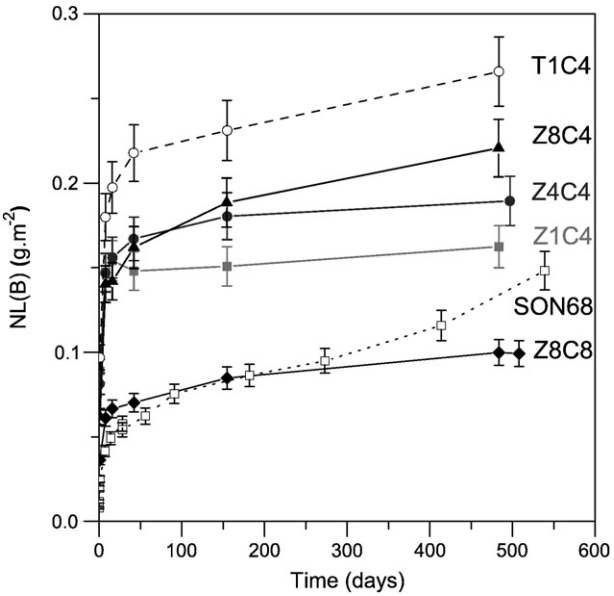

Fig. 4. Leaching kinetics of the Zr-bearing glasses and of the T1C4 compared to SON68 during alteration at $SA/V = 2000\ cm^{-1}$ and 90 °C in deionized water. Z1C4 (●), Z4C4 (■), Z8C4 (▲), Z8C8 (▼), T1C4 (○), and SON68 (□). $NL(B)$ of the SON68 alteration are taken from Frugier et al.[12].

Table 2
Rate, pH and rate drop factor measured during residual rate experiments (*SA*/*V* = 2000 cm^{-1} and T° = 90 °C). The residual rate of SON68 is recalculated for the same leaching period as the glasses investigated in this study.

Glass	r_r (g $m^{-2}d^{-1}$)	Std deviation	$pH_{90\ °C}$	r_0/r_r
Z1C4	3.3×10^{-5}	2.3×10^{-6}	9.63	1.0×10^{6}
Z4C4	4.4×10^{-5}	1.8×10^{-5}	9.53	3.3×10^{5}
Z8C4	1.2×10^{-4}	2.8×10^{-5}	9.35	3.2×10^{4}
Z8C8	5.8×10^{-5}	1.0×10^{-5}	9.21	7.3×10^{4}
T1C4	1.1×10^{-4}	2.6×10^{-6}	9.82	2.2×10^{5}
SON68	1.6×10^{-4}	1.4×10^{-5}	9.41	–

alteration shows that residual rate variations observed were due to variations in the diffusion properties of the gel. However, it is difficult to identify the mechanisms responsible for these residual rate variations. In the case of SON68 glass, increasing the pH decreases the diffusion coefficients of tracer elements in the gel [11]. The residual rate variation could therefore be attributed to an effect of the pH of the leaching solution.

3.4.2. Comparison between Zr and Ti

Although compositions differ only by the nature of the IVB element, T1C4 glass has a residual rate of 1.1×10^{-4} g $m^{-2}d^{-1}$ that is three times higher than Z1C4 (3.3×10^{-5} g $m^{-2}d^{-1}$). SEM observations of glass powders leached for 600 days do not reveal secondary crystalline phases in Zr-glasses. On the contrary, T1C4 contains a large amount of crystalline sodic-silicate phases, with a desert rose-like morphology (Fig. 5). XRD and SEM-EDS reveal the presence of magadiite ($Na_2Si_{14}O_{29}\cdot11H_2O$) [47]. The effect of Ti on r_0 and rate drop regimes suggests that Ti retains silicon less efficiently than Zr in the gel. This could lead to a higher SiO_2 concentration in the leaching solution, which will favor saturation with respect to magadiite.

Previous studies of SON68 glass have shown that the dissolution rate in the residual rate regime can be controlled by two mechanisms: the diffusion of water through the gel [11] and the precipitation of secondary crystalline phases formed by precipitation of elements from the solution at the gel/solution interface. The precipitation of these crystalline phases integrates some gel constituents leading to a lower concentration of these elements in the solution. This decrease of element concentration causes the dissolution of the gel leading to a partial loss of its protective properties [48]. In the case of SON68 glass alteration, these phases are mainly phyllosilicates containing Si, Ca, Al, Ni, Zn, and Fe [12]. The absence of Al in the studied glasses prevents the crystallization of phyllosilicates, allowing other phases to precipitate. As in the case of phyllosilicates, magadiite crystallizes from solution. The resulting decrease of SiO_2 concentration in the solution could explain the higher pH after 532 days of alteration of the T1C4 sample (9.82) compared to Z1C4 (9.63). As in the case of SON68, the precipitation of a secondary phase causes a decrease of the protective properties of the gel, explaining the difference between the residual rate of Z1C4 and T1C4.

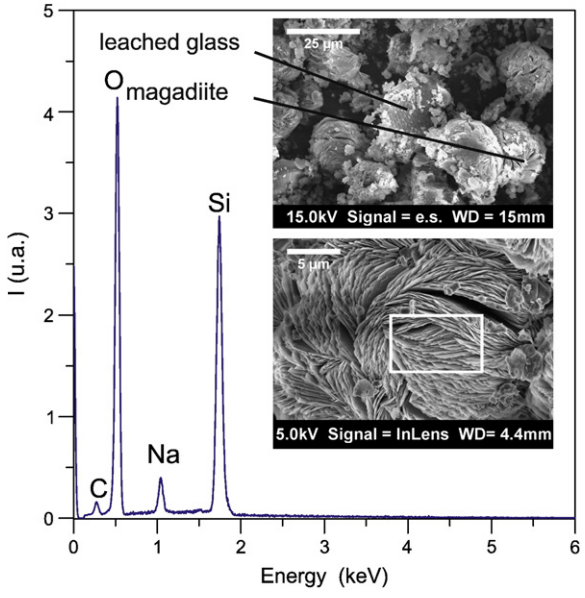

Fig. 5. SEM pictures and EDS analysis of T1C4 glass powder leached at 90 °C, *SA*/*V* = 2000 cm^{-1} during 600 days. (a) Overview of the leached glass powder and of the secondary crystalline phases. (b) Details of the secondary-phase morphology. The white frame corresponds to the scanned zone during the EDS analysis. EDS qualitatively confirms the presence of magadiite, $Na_2Si_{14}O_{29}\cdot11H_2O$.

3.4.3. CaO content

Z8C8 presents a residual rate twice lower than Z8C4 and a lower pH value of the alteration solution (9.21). Replacing Na_2O by CaO in glasses with high ZrO_2 content enhances gel protective properties. The addition of both Zr and Ca results in low residual rates and low pH values that can be seen as a benefit for gel durability.

4. Conclusion

The presence of IVB elements modifies the structure of soda-lime borosilicate glasses, with an decreasing proportion of $^{[4]}$B, due to competition for charge compensation between B and Zr, Hf or Ti. Similar values of $^{[4]}$B proportion indicate a similar 6-coordination of Zr, Hf or Ti, except for the glasses with 8 mol% TiO_2 in which $^{[4]}$B proportion is consistent with $^{[5]}$Ti. A major conclusion of this study is the evidence of a decrease of r_0 by about 1 order of magnitude when increasing ZrO_2 and HfO_2 up to 8 mol%. The evolution of r_0 with the presence of TiO_2 and CaO arises from specific structural properties of Ti during hydrolysis. The variation of glass composition modifies the glass structure, leading to changes in the concentration of hydrolysable bonds. A better structural understanding of the glass and interphase will help rationalizing the effect of glass composition on r_0.

Glasses with the highest r_0 values also exhibit a rapid decrease in their dissolution rate after a few days, regardless of the IVB element, in agreement with Monte-Carlo simulations [10]. However, the case of T4C4 glass highlights that the slowdown of the dissolution rate is not only controlled by the concentration of IVB elements but also by their ability to prevent the SiO_2 dissolution by a change in their local environment.

The role of IVB elements is different during the initial dissolution rate and the residual rate regime, as shown by the increase in the residual rate when increasing the Zr content of the glass. A faster residual dissolution rate is observed in the 1 mol% TiO_2 glass, due to the formation of a secondary crystalline phase. This highlights the synergy between IVB elements and the other gel components (Si, Ca, and Na) with a major role played by local charge compensation. Our study confirms that the only use of r_0 does not allow the prediction of long-term behavior of glasses for high-level waste containment. A monitoring of the structural properties of IVB elements during glass alteration may shed light on the origin of their influence on glass durability, as demonstrated on other glasses [10,14].

Acknowledgments

The authors are grateful to Imène Machouk (IMPMC) for her help on SEM experiments and Yves Minet (CEA-Marcoule) for the comments.

References

[1] S. Gin, N. Godon, I. Ribet, P. Jollivet, Y. Minet, E. Vernaz, J.M. Cavedon, B. Bonin, R. Do Quang, Mater. Res. Soc. Symp. Proc. 824 (2004) 327.
[2] Z. Boksay, G. Bouquet, S. Dobos, Phys. Chem. Glasses (1968) 69.
[3] G. Geneste, F. Bouyer, S. Gin, J. Non-Cryst. Solids 352 (2006) 3147.
[4] R.H. Doremus, J. Non-Cryst. Solids 19 (1975) 137.
[5] L. Sicard, O. Spalla, F. Né, O. Taché, P. Barboux, J. Phys. Chem. C 112 (2008) 1594.
[6] P. Frugier, S. Gin, Y. Minet, T. Chave, B. Bonin, N. Godon, J.-E. Lartigue, P. Jollivet, A. Ayral, L. De Windt, G. Santarini, J. Nucl. Mater. 380 (2008) 8.
[7] B. Grawbow, Mater. Res. Soc. Symp. Proc. 44 (1985) 15.
[8] F. Delage, D. Ghaleb, J.L. Dussossoy, O. Chevalier, E. Vernaz, J. Nucl. Mater. 190 (1992) 191.
[9] P. Jollivet, F. Angeli, C. Cailleteau, F. Devreux, P. Frugier, S. Gin, J. Non-Cryst. Solids 354 (2008) 4952.
[10] C. Cailleteau, F. Angeli, F. Devreux, S. Gin, J. Jestin, P. Jollivet, O. Spalla, Nat. Mater. 7 (2008) 978.
[11] T. Chave, P. Frugier, A. Ayral, S. Gin, J. Nucl. Mater. 362 (2007) 466.
[12] P. Frugier, S. Gin, J.E. Lartigue, E. Deloule, Mater. Res. Soc. Symp. Proc. 932 (2006) 305.
[13] M. Arab, C. Cailleteau, F. Angeli, F. Devreux, L. Girard, O. Spalla, J. Non-Cryst. Solids 354 (2008) 155.
[14] E. Pelegrin, G. Calas, P. Ildefonse, P. Jollivet, L. Galoisy, J. Non-Cryst. Solids (2010), doi:10.1016/j.jnoncrysol.2010.02.022.
[15] G. Calas, L. Cormier, L. Galoisy, P. Jollivet, C.R. Chim 831 (2002).
[16] E.B. Watson, Contrib. Mineral. Petrol. 70 (1979) 407.
[17] L.L. Davis, J.G. Darab, M. Qian, D. Zhao, C.S. Palenik, H. Li, D.M. Strachan, L. Li, J. Non-Cryst. Solids 328 (2003) 102.
[18] T. Kobayashi, J. Nucl. Sci. Technol. 44 (2007) 90.
[19] D. Rai, Y.X. Xia, N.J. Hess, D.M. Strachan, B.P. McGrail, J. Solution Chem. 30 (2001) 949.
[20] G. Ferlat, L. Cormier, M.H. Thibault, L. Galoisy, G. Calas, J.M. Delaye, D. Ghaleb, Phys. Rev. B 73 (2006) 214207.
[21] L. Galoisy, E. Pelegrin, M.A. Arrio, P. Ildefonse, G. Calas, D. Ghaleb, C. Fillet, F. Pacaud, J. Am. Ceram. Soc. 82 (1999) 2219.
[22] X.C. Yang, M. Dubiel, D. Ehrt, A. Schuetz, J. Non-Cryst. Solids 354 (2008) 1172.
[23] F. Farges, G.E. Brown, J.J. Rehr, Geochim. Cosmochim. Acta 60 (1996) 3023.
[24] L. Cormier, P.H. Gaskell, G. Calas, A.K. Soper, Phys. Rev. B 58 (1998) 11322.
[25] C. Lopez, X. Deschanels, C. Den Auwer, J.-N. Cachia, S. Peuget, J.-M. Bart, Phys. Scr. T115 (2005) 342.
[26] O. Dargaud, G. Calas, L. Cormier, L. Galoisy, C. Jousseaume, G. Querel, M. Newville, J. Am. Ceram. Soc. 93 (2010) 342.
[27] D. Massiot, C. Bessada, J.P. Coutures, J. Virlet, F. Tautelle, J. Magn. Reson. 231 (1990) 90.
[28] F. Angeli, M. Gaillard, T. Charpentier, P. Jollivet, J. Non-Cryst. Solids 354 (2008) 3713.
[29] L. Wüllen, W. Müller-Warmuth, Solid State Nucl. Magn. Reson. 2 (1993) 279; P.K. Abraitis, B.P. McGrail, D.P. Trivedi, F.R. Livens, D.J. Vaughan, J. Nucl. Mater. 280 (2000) 196.
[30] F. Angeli, T. Charpentier, D. de Ligny, C. Cailleteau, J. Am. Ceram. Soc. (In press); DOI: 10.1111/j. 1551-2916.2010.03771.x.
[31] L.S. Du, J.F. Stebbins, J. Phys. Chem. B 107 (2003) 10063.
[32] G.L. Turner, K.A. Smith, R.J. Kirkpatrick, E. Oldfield, J. Magn. Reson. 67 (1986) 544.
[33] L. Cormier, D. Ghaleb, J.M. Delaye, G. Calas, Phys. Rev. B 61 (2000) 14495.
[34] S. Gin, C. Jegou, Water Rock Int. Proc. (2001) 279.
[35] X. Feng, A. Barkatt, Mater. Res. Soc. Symp. Proc. 112 (1988) 543.
[36] X. Feng, T.B. Metzger, Mater. Res. Soc. Symp. Proc. 432 (1997) 27.
[37] A. Paul, J. Mater. Sci. 12 (1977) 2246.
[38] C.M. Jantzen, M.J. Plodinec, J. Non-Cryst. Solids 67 (1984) 207.
[39] S.U. Aja, M.D. Dyar, Appl. Geochem. 10 (1995) 603.
[40] H.S.C. O'Neill, Am. Mineral. 91 (2006) 1134.
[41] J.D. Rimstidt, H.L. Barnes, Geochim. Cosmochim. Acta 44 (1980) 1683.
[42] D. Tromans, J. Nucl. Mater. 357 (2006) 221.
[43] I. Gunnarsson, S. Arnorsson, Geochim. Cosmochim. Acta 64 (2000) 2295.
[44] F. Angeli, M. Gaillard, P. Jollivet, T. Charpentier, Geochim. Cosmochim. Acta 70 (2006) 2577.
[45] B.C. Bunker, J. Non-Cryst. Solids 179 (1994) 300.
[46] B.E. Scheetz, W.P. Freeborn, K.S. Deane, C. Anderson, M. Zolensky, W.B. White, Mater. Res. Soc. Symp. Proc. 44 (1985) 129.
[47] G.G. Almond, R.K. Harris, K.R. Franklin, J. Mater. Chem. 7 (1997) 681.
[48] S. Ribet, S. Gin, J. Nucl. Mater. 324 (2004) 152.